3 1176 01306 6965

$N 86 - 17703$

$NASA CR-178474$

NASA-CR-178474
19860008233

FINAL REPORT

Prepared for

GEORGE C. MARSHALL SPACE FLIGHT CENTER
MARSHALL SPACE FLIGHT CENTER
ALABAMA   35812

CONTRACTOR:	Desert Research Institute Atmospheric Sciences Center University of Nevada System P.O. Box 60220 Reno, NV 89506
TITLE OF CONTRACT:	Evaluation of Data Obtained from Atmospheric Laser Doppler Velocimeter
DATE OF THIS REPORT:	June 20, 1985
CONTRACT NO.:	NAS8-34731
AUTHORS:	Thomas S. Keck and James W. Telford

NF00204

1. Introduction

The doppler lidar velocimeter produces a variety of kinds of data. Besides the line of sight velocity components, there are the reflected amplitudes and the doppler widths. The work done under this contract has produced computer graphics software for displaying these data. Different methods of presentation are needed for the various items. The overall goal is to produce a picture as pictures are often the best way to gain understanding. The individual lidar scans form a crosshatch pattern. Thus one-dimensional measurements fit together to form a two-dimensional whole. A pair of velocity measurements at a point combine to form a wind measurement with direction and magnitude. This gives a forest of wind vectors. The goal is to find a recognizable pattern to these "trees." Often it is necessary to show only part of the information. That is, show only the wind direction not its magnitude or reduce the wind to streamlines of air flow. In other cases data are reduced to contour plots. Just enough contour lines are included to show the picture that the text of this report is trying to describe. These data do not change smoothly and contour lines can become so closely spaced that the plotter ink runs individual lines into a black mass.

Most of the plots in this report use a 500 meter grid. This was chosen as fine enough to show detail yet coarse enough that the mesh of the lidar scans does not miss many grid points. Even so there are isolated grid points with no data yet most of their neighbors are covered. These points caused considerable clutter

in the contour plots until they were given data values just the average of their neighbors. In a few cases the grid spacing was increased to 600 meters, but this was only done when computer memory limits were exceeded. The coordinate system of these plots is based with its (0,0) point at the start of a data collection run. There are two runs each with its own starting point. Labels are given in kilometers with north upward and east to the right. The quantity SIGMA requires some explanation. This gives the standard error estimate of a velocity measurement. It depends on the signal to noise ratio of the reflected signal. A weak signal becomes lost in the noise and so deserves a large uncertainty in its velocity estimate. The formula used is due to Bob Lee of Lassen Research and is given by

$$\text{SIGMA} = (0.025Q(1 + .08Q))^{-1/2}$$

where Q is the signal power divided by the noise power. The noise was estimated from the average signal amplitude in the 20 readings farthest from the aircraft in each scan. The data tape included both raw doppler velocities and smoothed velocities. The raw velocity measurements rather than the smoothed ones are used except in the one case noted below. Velocity estimates from a pair of scans are made as if both occurred at the same time. That is, no attempt was made to "advect" the data or adjust for air motion in the time interval between the two measurements. This is reasonable since the winds measured at the aircraft, not

using the lidar, vary smoothly. See for example the wind vectors on Fig. 8. The winds seem steady and slowly varying. This gives some confidence in combining wind components measured at different times.

2. Doppler Measured Winds

First let us look at the overall character of the winds measured by the lidar. The figures included here show only wind magnitudes. The wind vectors need to be so small that one could not distinguish their length given the thickness of the lines drawn. In any case, the direction of the arrowheads is enough for the points made here. Compare Figs. 1 and 2 which show the winds computed for the circuit of the first cloud. Fig. 1 shows winds at every point for which there is data. A grid point must have at least 2 scans to compute a wind. Fig. 2 shows the highest quality data for which the uncertainty, sigma, is less than 2 m/s. (Sigma is limited by software to values less than 32.) Most of the data of Fig. 1 is thrown away in Fig. 2. The data that remains is near turns. Data in turns is somewhat suspect. Delays in the inertial navigation system made it difficult to aim the lidar during turns. So it is not clear that the lidar is pointing level to the ground during turns. Hence two crossing scans may actually not intersect the same air parcel. The situation in the second cloud pass is somewhat better. Fig. 3 is an uncritical display of all the data and Fig. 4 is

limited to the best data with sigma less than 2 m/s. A considerable amount of data remains in the southwest part of the area. Is is with this region that we will later concentrate. Wind directions seem to stay constant over large regions and change suddenly at the boundary with other regions. This is most clear in Figs. 1 and 3. It is also noticeable in Fig. 2 around 30 km north and in Fig. 4 around 3 km north of start. Fig. 5 shows data with sigma less than 8 m/s. Starting at the southern flight path around 30 km west of start the arrowheads point uniformly at first but more and more are pointed at odd angles as the distance from the airplane increases. Around 37 km west and 13 km north of start is an area of randomly pointing wind directions. Most of these have sigma between 4 and 8 m/s. The wind speed at the airplane near there is a steady 24 m/s outside the turn. This is enough larger than sigma that the lidar may actually be detecting turbulent air motion in this region. Certainly the direction can stay much more uniform with the same quality of data, e.g. in the southern part of the area mentioned above.

3. Cloud Boundaries

Now let us focus on the idea of using the lidar to outline the boundary of a cloud. The absorption of the laser beam should increase dramatically when it enters cloudy air. This should show up clearly in the recorded data. Because of better data

coverage the second cloud starting at 17:44:09 was chosen for analysis here. Figs. 6 and 7 are taken from the photographic flight record. These black and white reproductions are less clear than the sequence of color originals. They are included here for quick reference. Fig. 6 gives a sideward view of the growing end of a cumulus cloud taken at 17:50:08. The edges are sharply defined and the cloud continues to the right out of the picture in the direction of flight. Fig. 7 taken at 17:53:13 shows the anvil top of the same cloud. This is the dissipating end of the cloud. The cloudy air below the anvil has no sharp boundaries. These two times are marked in Fig. 8. This is a contour plot of the signal to noise ratio. When more than one scan goes through a point, the one with the greatest reflected amplitude is chosen. Only two contour levels have been drawn for clarity. The outer one is at 4 db and the inner one is 10 db higher at 14 db. The region left and just below center shows a sudden drop in the reflected signal a few kilometers from the aircraft. It often drops a factor of 10 in less than 500 m, the grid size in this plot. This is what would be expected at the cloud boundary. The view from the aircraft at 17:50:08 looks part way up the growing face of the cloud. A right angle drawn from the flight path extends through the inside edge of the low reflecting region. At 17:53:13 the camera sees cloud with ill-defined boundaries. The lidar shows patches of reflective area

without sharp edges. The space between the 4 db and 14 db levels is much larger. Thus the lidar gives us a picture consistent with a cloud boundary.

The doppler width also shows some effects near the conjectured cloud boundary. This quantity measures how the velocity varies over a short section of the beam, i.e. it measures turbulence. Once the beam passes the cloud edge, very little signal is returned. This effectively shortens the distance over which the turbulence is measured. Thus doppler width should be lower for a section of the beam that is part way into the cloud. Fig. 9 shows the areas where there is large reflected signal (low sigma). The doppler widths should be most accurate in those areas. Fig. 10 singles out from Fig. 9 those areas with low doppler width. When Fig. 9 is laid over Fig. 10, it is seen that many of the low width areas are exactly at the edge of the area of good reflectivity. Now low sigma is the same as high signal to noise ratio. This is the same as the cloud boundary chosen before. 2 m/s corresponds to about 8 db.

Fig. 11 shows the same effect with the high doppler width areas. As before the doppler width should be underestimated right at the cloud edge. Thus points with higher turbulence may appear to have lower doppler width when they are right at cloud boundary. Thus some of these may be excluded from Fig. 11. Overlaying Fig. 9 on Fig. 11 seems to show a lack of high width

areas right on the supposed cloud boundary. The points on the border that do show high doppler width seem to be mostly part of larger areas of turbulence.

4. Airflow from Doppler Winds

Two regions were selected for computing airflow. The first was selected from Fig. 2. It is shown in Fig. 12. The stream-lines show a kink near 2 km east and 29 km north of start. This is at the boundary between 2 different regions showing their own nearly constant winds. This was mentioned above in the discussion of winds. Fig. 13 selects the best region for winds from Fig. 4. The wind makes some strange corners in the vicinity of the turn. The problems with winds in turns was mentioned above.

5. Comparison of Aircraft and Lidar Winds

The winds measured at the aircraft provide an independent check of the values derived from the lidar. To give both systems the opportunity to produce the best data, segments of straight and level flight were chosen. The nearest points to the flight path with lidar winds were selected to do the comparison. The results are shown in Table 1. The two winds compare moderately well. The wind directions agree within 15°. The same com-putations were done using the smoothed velocities that were pro-vided on the data tape. These are shown in Table 2. The

velocity agreement was not as good in all but one case. This is one reason that the smoothed velocities were not used elsewhere. Another reason is that smoothing will tend to hide turbulence. Turbulence was one of the things we hoped to study.

6. Conclusions

The doppler lider seems successful at producing at least qualitative pictures of airflow from long distances. The principal weakness seems to be the strength of the reflected signal. Its amplitude is often no more than the noise coming from the instrument and from the environment. The environmental noise comes from the ambient level of illumination at the laser frequency and cannot be helped. Instrument noise depends on the state of the art, but the two cannot be separated here. One could choose to operate the lidar when there is increased backscatter from the beam, i.e. when there is air pollution. Thus one could look at air and clouds in polluted urban areas. A second possibility would be to examine the storms that arise in the smokey plumes above forest fires. In the present case one cloud produced much better data than the other. This shows that there is room for the aircraft crew to seek out clouds that are surrounded by air with ample backscatter.

The lidar was most successfully used here as a ranging device. The lasar scans in the horizontal can give an outline of a horizontal slice of a cloud. If the beam were directed above

and below the plane of flight, one could outline the whole sur-
face of the cloud. A series of cloud scans could follow the evo-
lution of a single cloud. This would mean giving up the ability
to measure wind vectors over the 500 meter grid used here. Most
of the scans would be done at directions above or below the hori-
zontal. This would be a better job for a simpler instrument
without the ability to measure doppler shifts.

It seems clear that if the instrument is to be used to sup-
port scientific studies aimed at elucidating important scientific
questions, then the instrumentation will need to be under the
guidance of a scientific director with a good record of airborne
research discoveries in cloud physics, other instruments which
can be used to gather information about the cloud interior will
need to be added and used to supplement the air motion measure-
ments, and the aircraft will need to be dedicated to such a spe-
cific mission for about a month at a time, once a year, for
several years.

Unsmoothed Lidar Data

Time Interval	Number of Points	Average Wind		Average Lidar Wind		Difference in Direction
		East	North	East	North	
17:34:10 17:35:30	15	25	-7	17	-10	15°
17:45:55 17:48:03	16	21	-6	17	-8	9°
17:48:50 17:50:18	5	24	-6	21	-11	14°
17:51:31 17:54:14	10	18	-6	19	-12	14°
17:55:59 17:58:28	70	22	-7	20	-9	7°

Table 1: This compares the winds measured at the airplane with lidar winds computed for points near the aircraft. The unsmoothed lidar velocities are used.

Smoothed Lidar Data

Time Interval	Number of Points	Average Wind East	North	Average Lidar Wind East	North	Difference in Direction
17:34:10 17:35:30	15	25	-7	16	-10	16°
17:45:55 17:48:03	16	21	-6	-10	-10	119°
17:48:50 17:50:18	5	24	-6	21	-15	22°
17:51:31 17:54:14	10	18	-6	22	-12	10°
17:55:59 17:58:28	70	22	-7	14	-8	12°

Table 2: This compares the winds measured at the aircraft with smoothed lidar winds. Lidar winds are measured near the aircraft.

14JUL81 FROM 17:31:32 TO 17:41:37

WIND DIRECTION
SIGMA<32.0
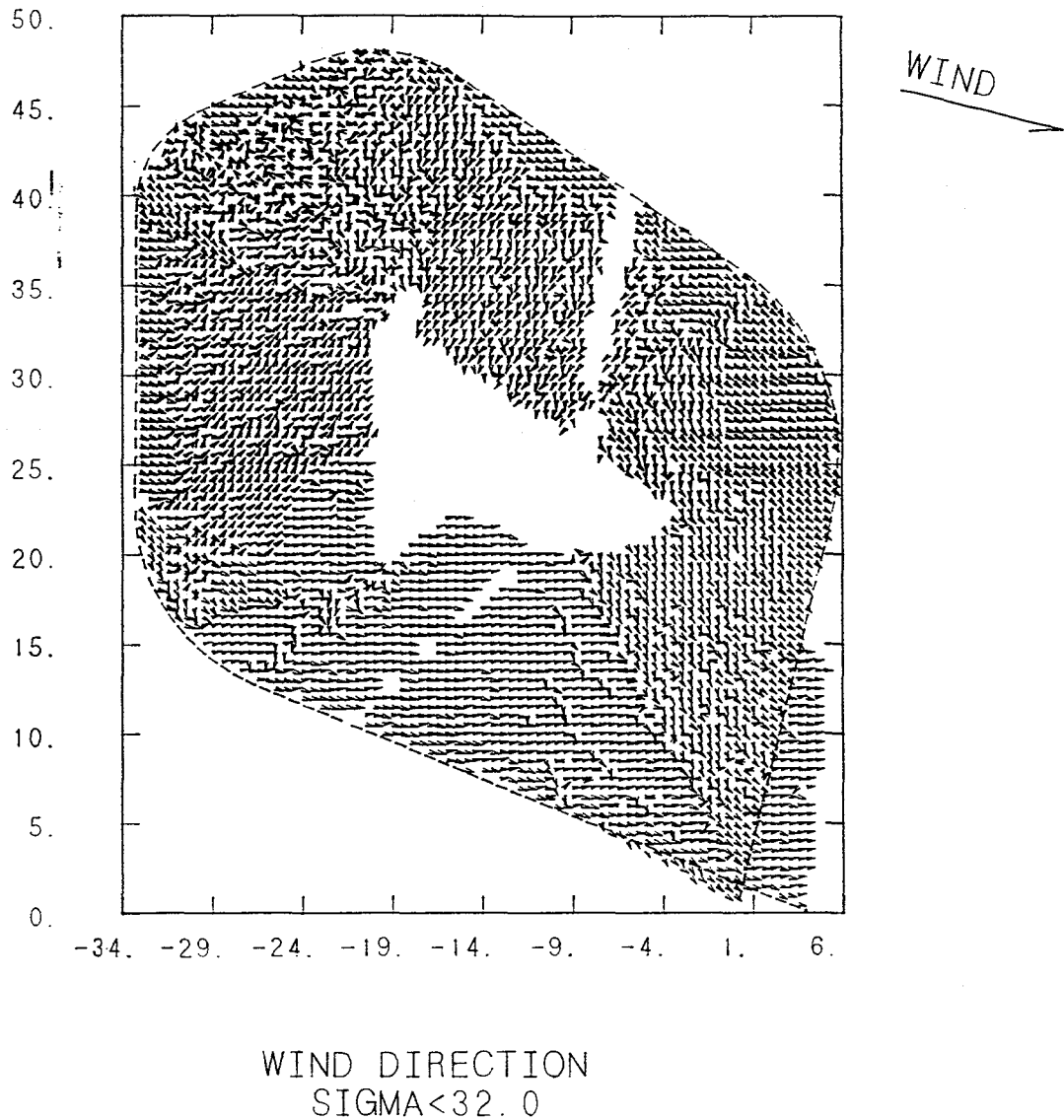
Fig. 1. All measured wind directions are shown for the first cloud circuit. Winds are accepted even if their uncertainty reaches the largest value of nearly 32 m/s. The single wind vector of 22 m/s in the upper right was measured at the airplane at the beginning of the data. Labels show distance in kilometers from start of data. The dashed line shows the flight path of the airplane.

14JUL81 FROM 17:31:32 TO 17:41:37
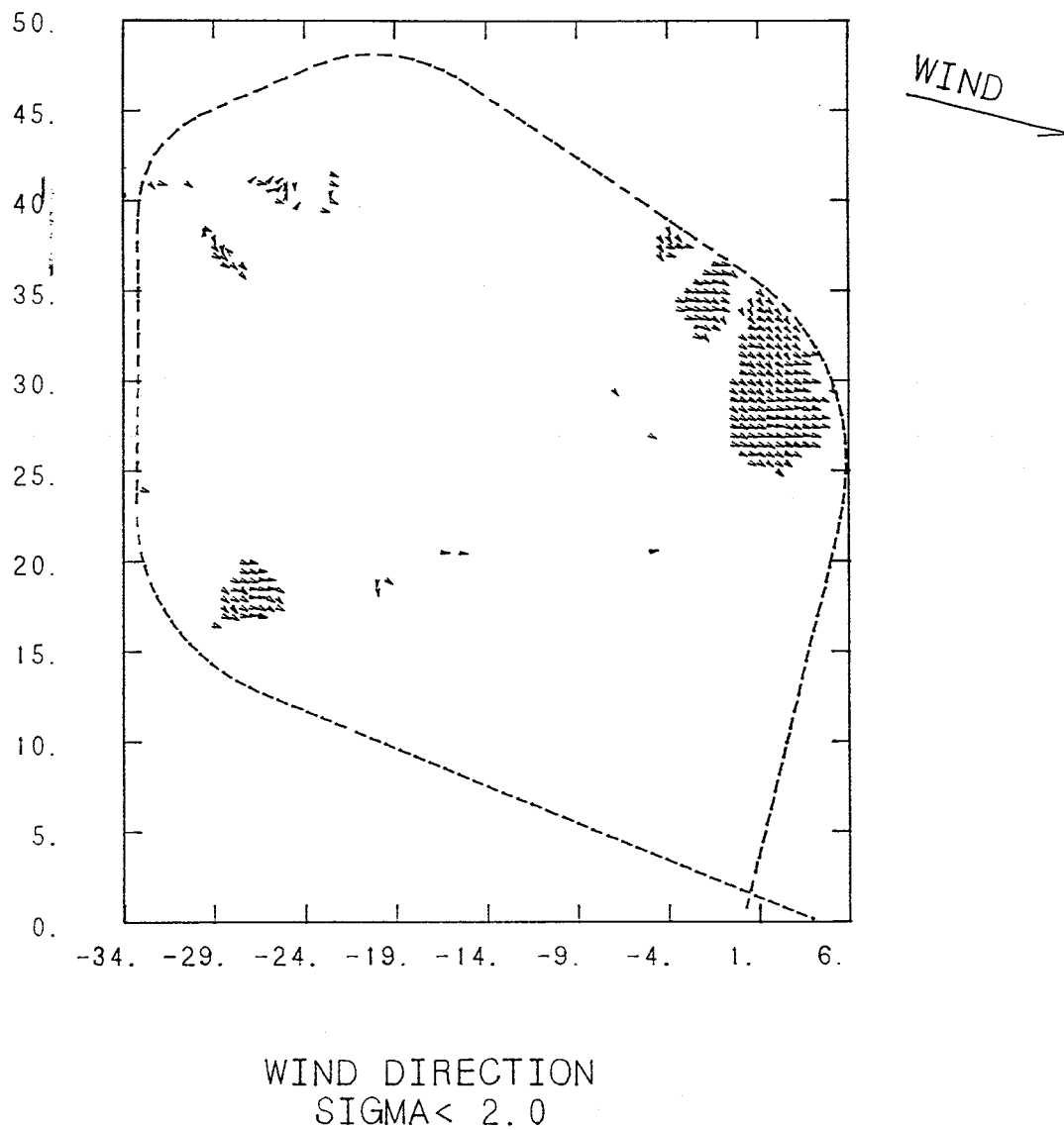
Fig. 2. These are wind directions from the first cloud circuit. All winds with uncertainty sigma, greater than 2 m/s have been deleted.
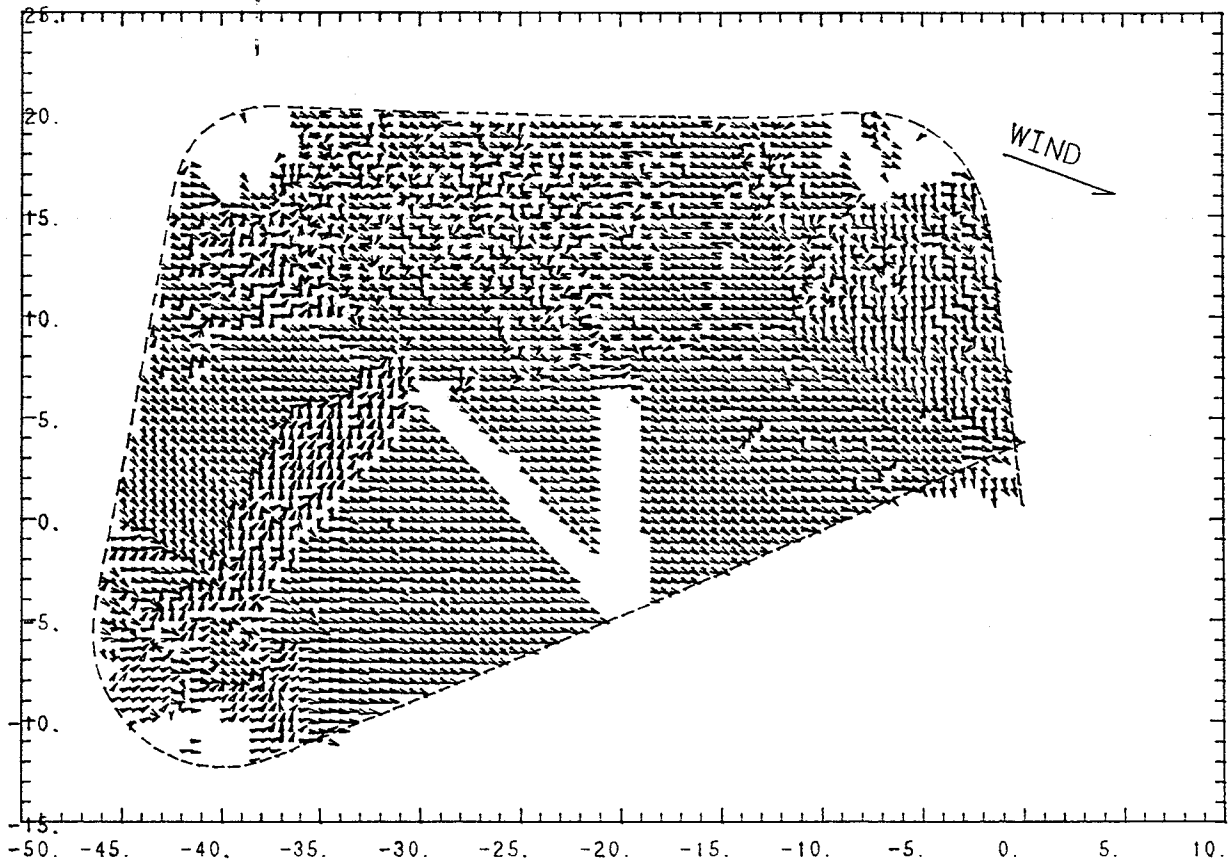
WIND DIRECTION
SIGMA<32.0

Fig. 3. This shows all wind vectors measured for the circuit about the second cloud.
The single wind vector 19 m/s was measured at the airplane. The dashed
line shows the flight path.
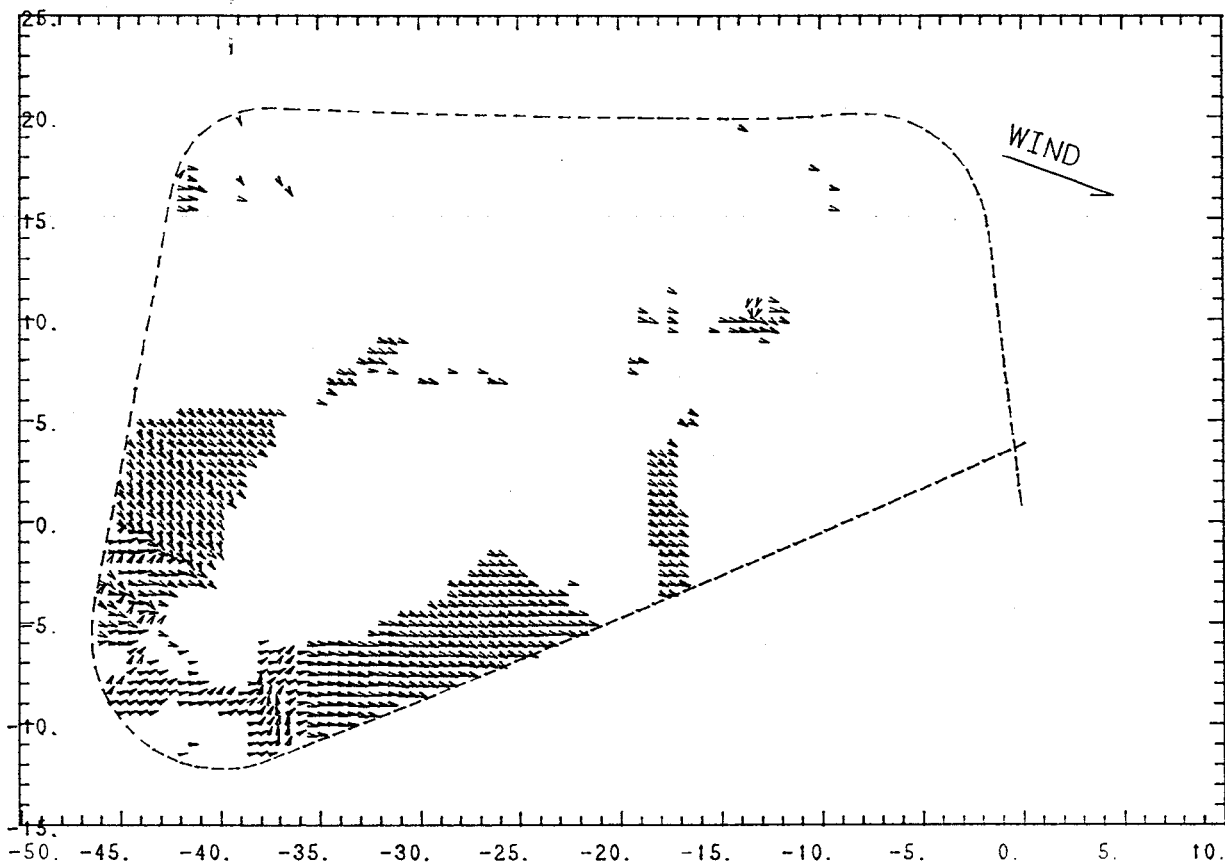
WIND DIRECTION
SIGMA< 2.0

Fig. 4.   This shows the directions of the wind vectors with smallest uncertainty for the second cloud circuit. The southwest portion of data is used for further analysis.

14JUL81 FROM 17:44:09 TO 17:54:14
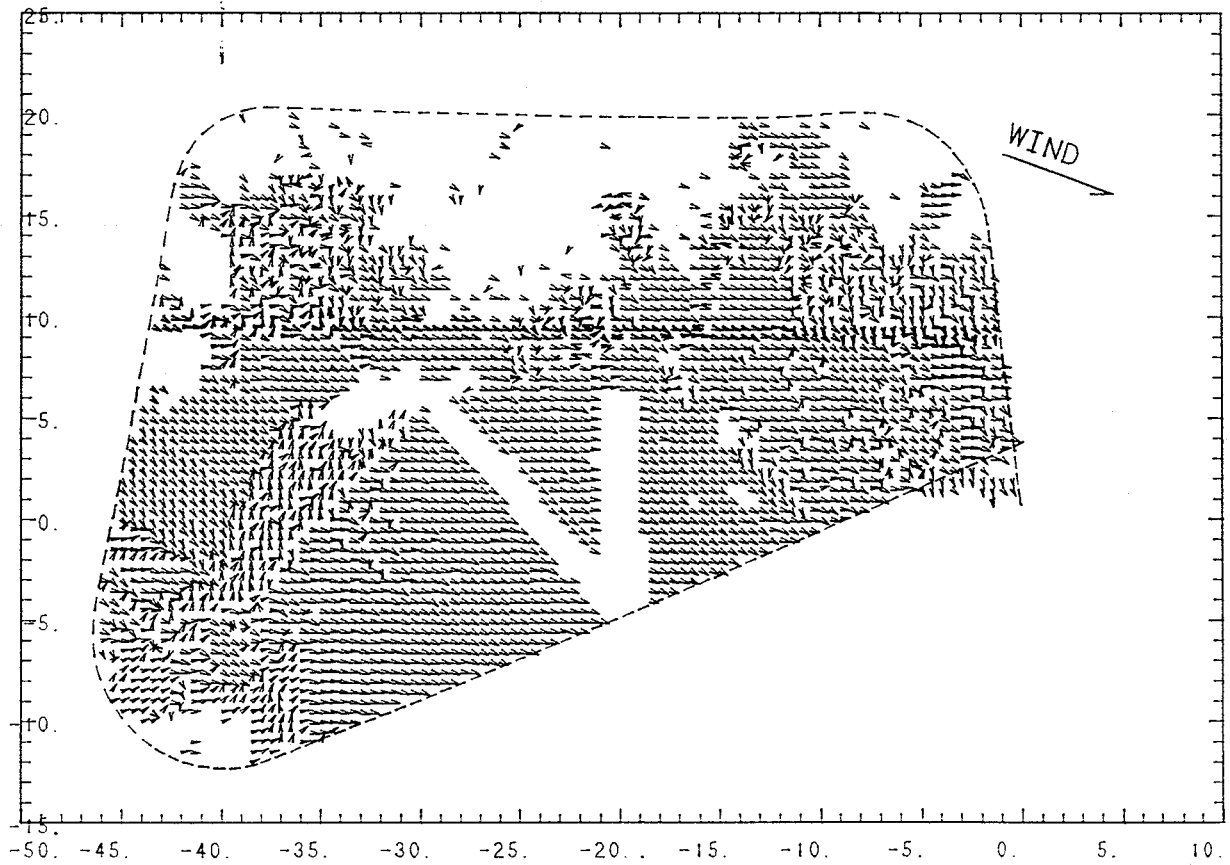
WIND DIRECTION
SIGMA< 8.0

Fig. 5.   This shows the data of Fig. 3 with the data of uncertainty 8 m/s or more removed.   The region around 37 km west and 13 km north of start may be a pocket of turbulent air.
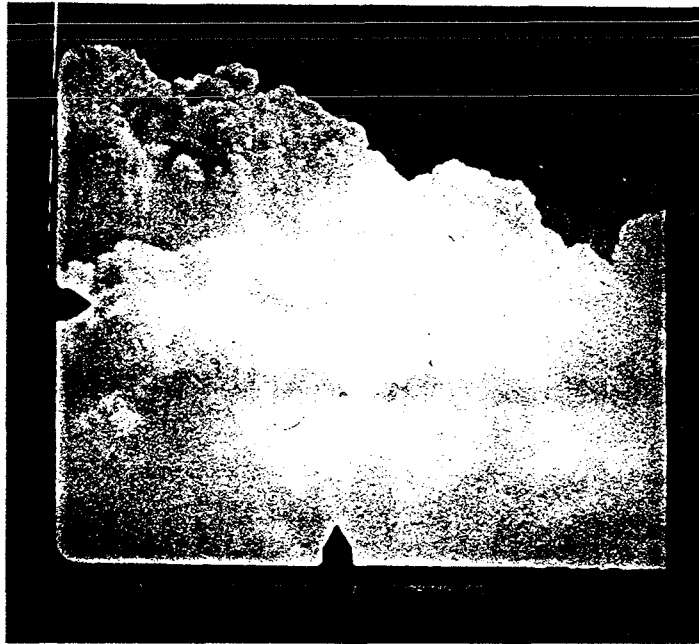
Fig. 6. This picture from the photographic flight record at 17:50:08 shows the
sharp boundary of the growing end of the cumulus cloud.

Fig. 7. This photograph was taken later at 17:53:13 shows the anvil top of the
same cloud.

14JUL81 FROM 17:44:09 TO 17:54:14
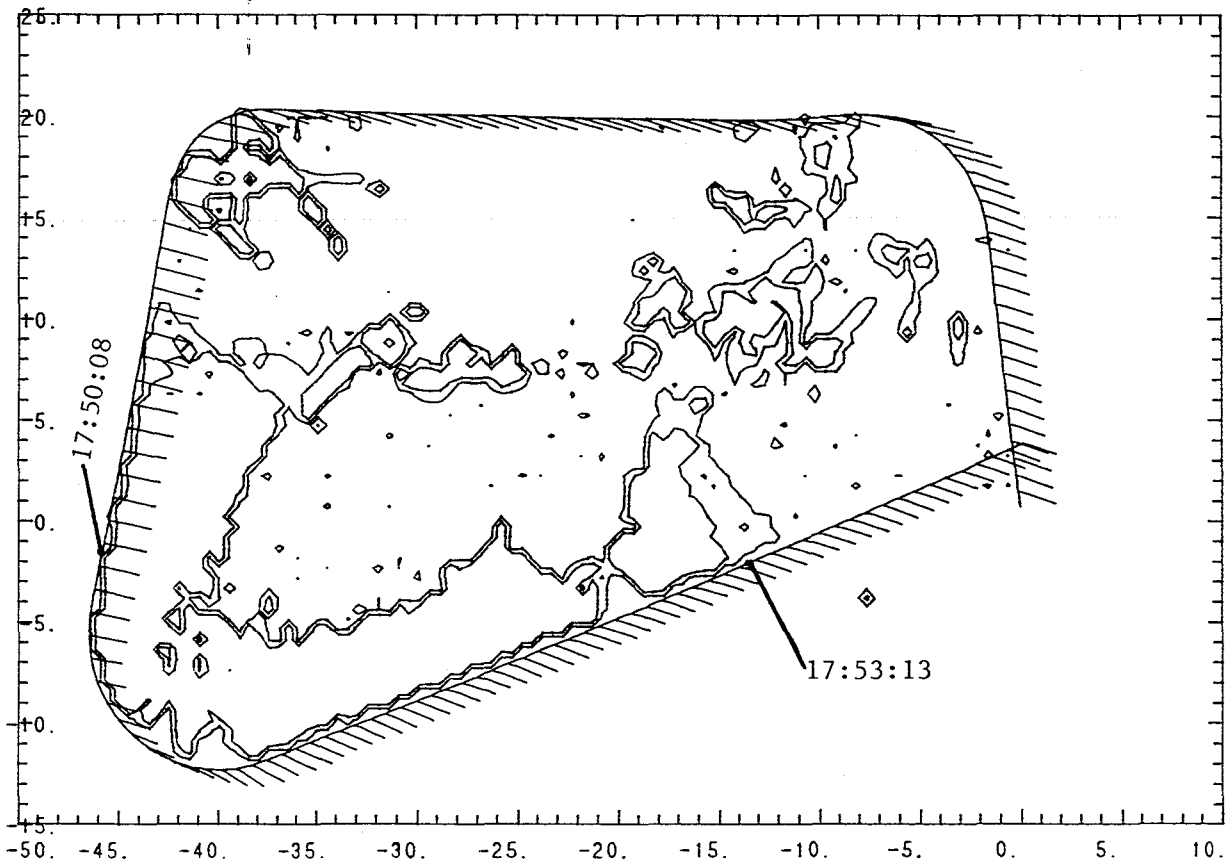
SIGNAL TO NOISE RATIO (DB)

CONTOUR FROM 4.0000 TO 14.000 CONTOUR INTERVAL OF 10.000

Fig. 8. This shows the signal to noise ratio. The outer contour lines surround areas with reflection at least 4 db above the noise. The inner lines are 10 db higher with 14 db returned. The flight path is shown with wind vectors averaging 20 m/s.
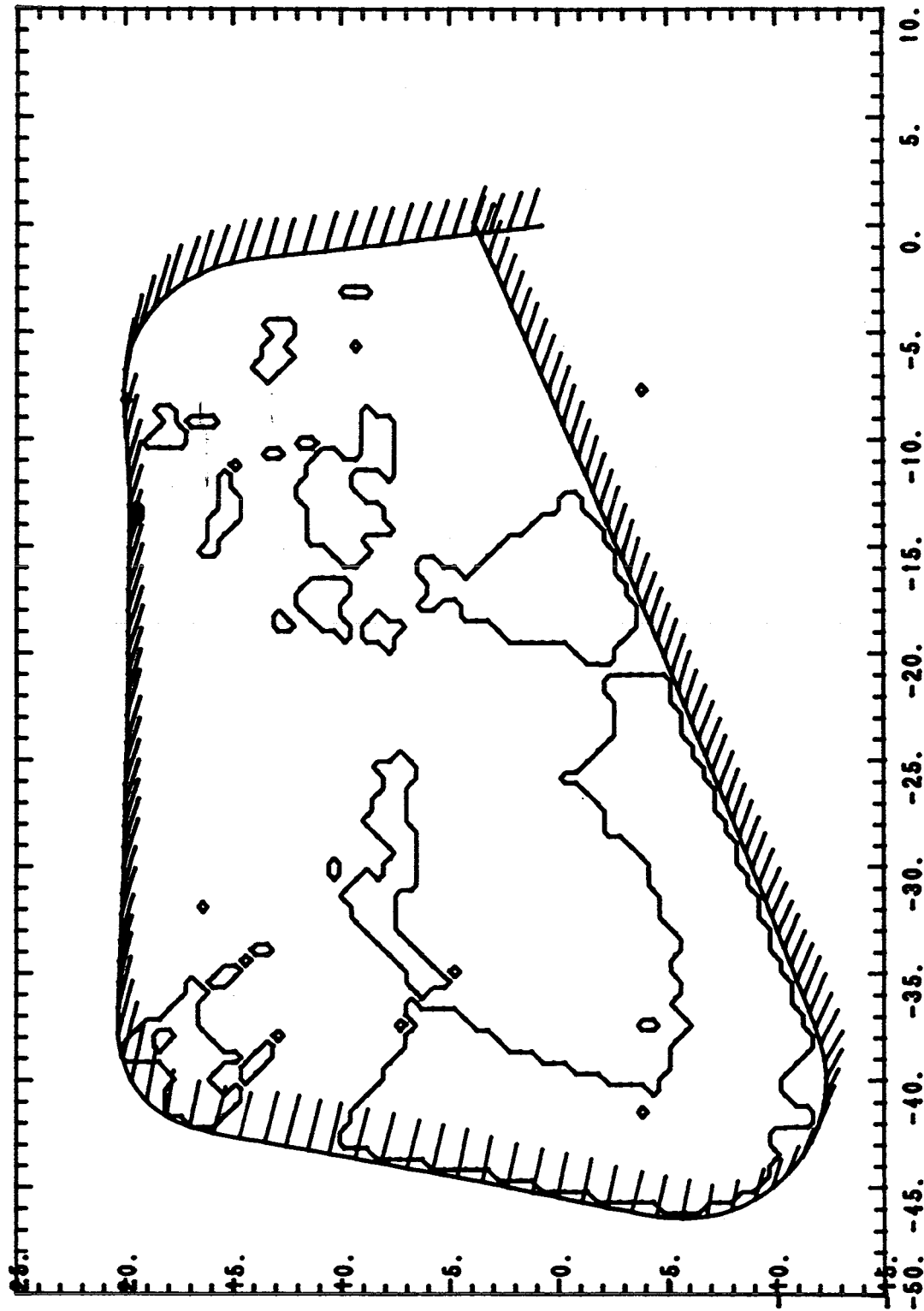
Fig. 9. The curves in this plot surround the areas of doppler width data with sigma less than 2 m/s. Use this plot to indicate the areas where data are available. 0.1 to 15 includes the full range of doppler widths.
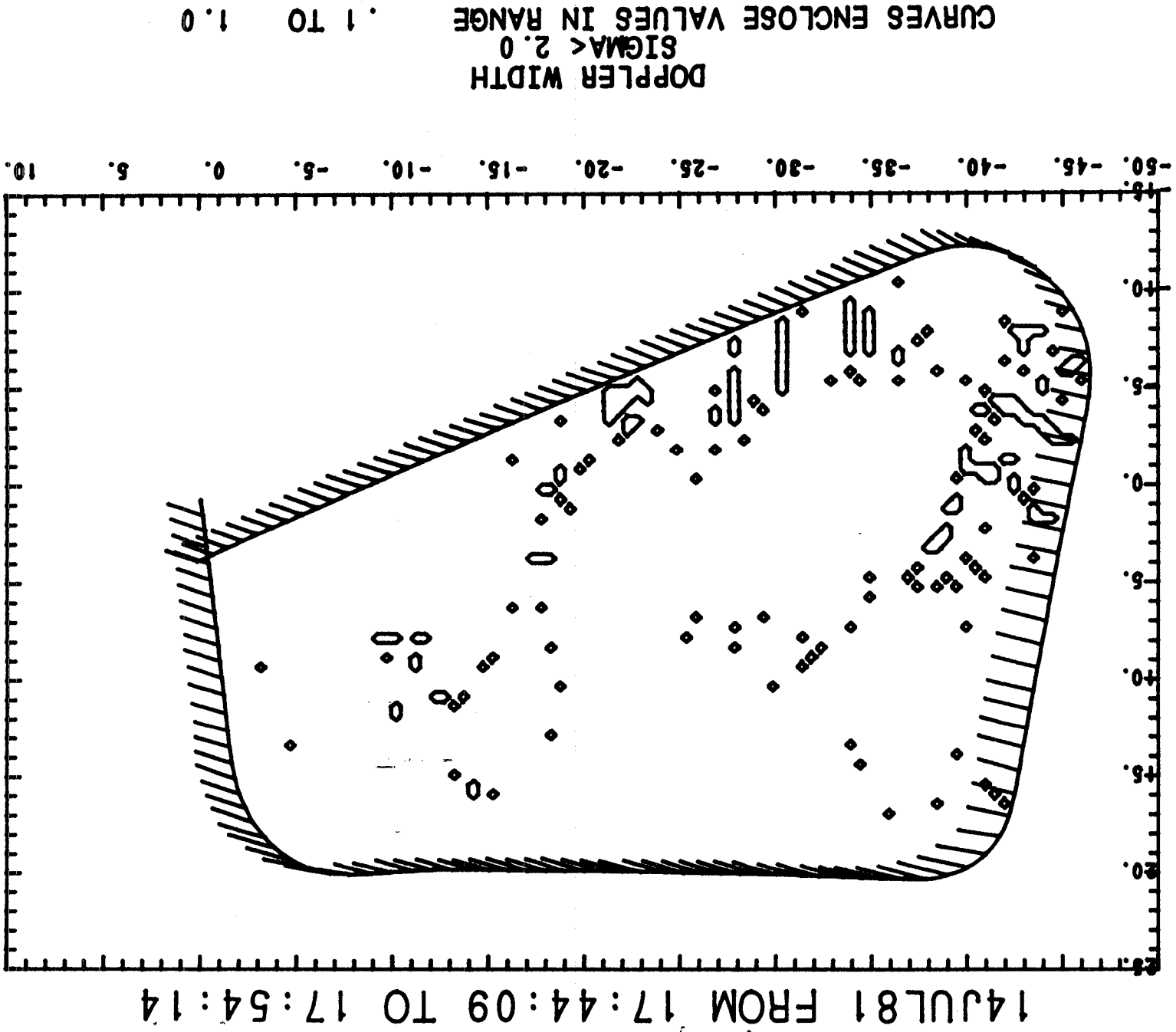
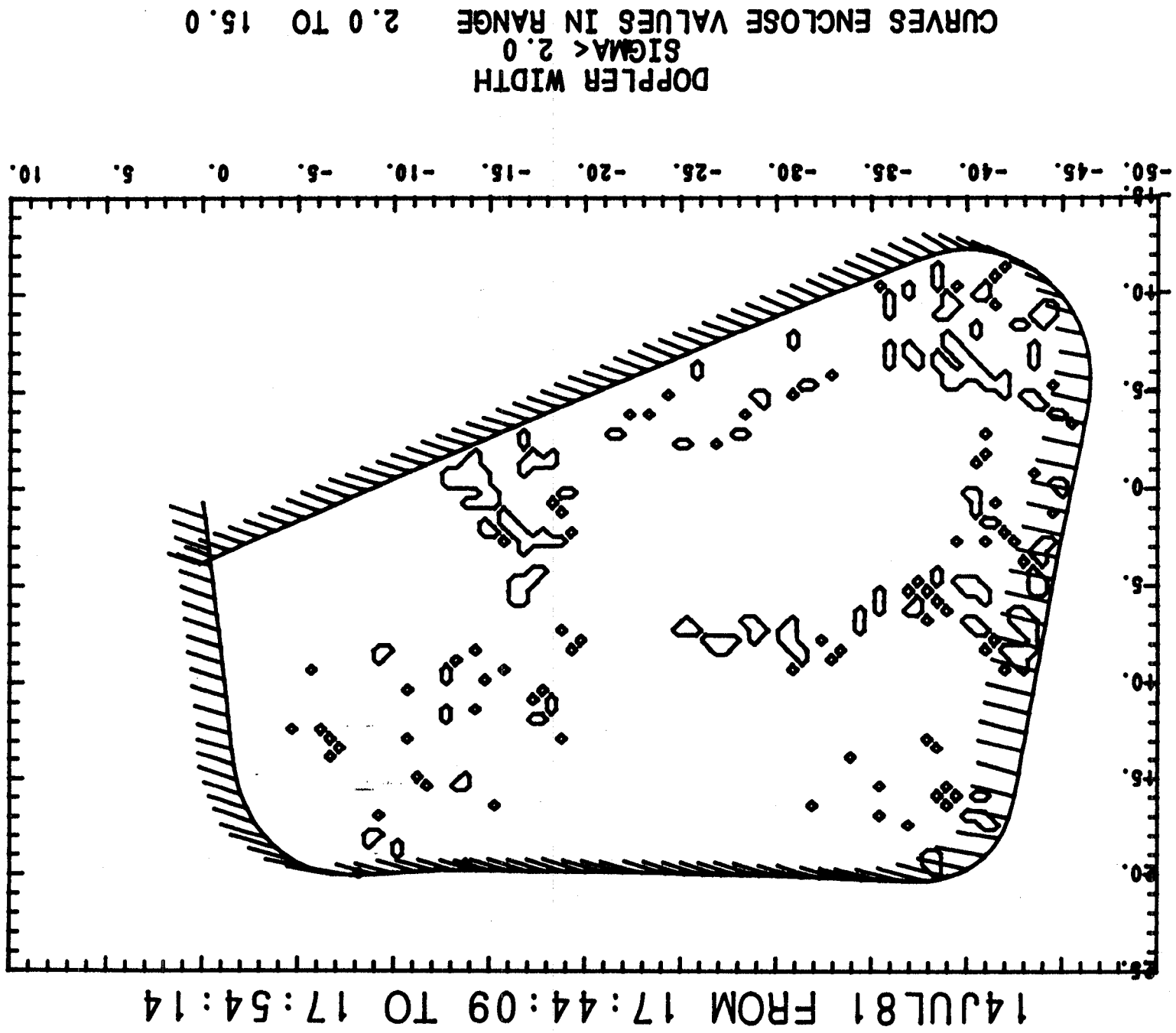Fig. 10. The curves in this plot surround areas in which the doppler width is low.
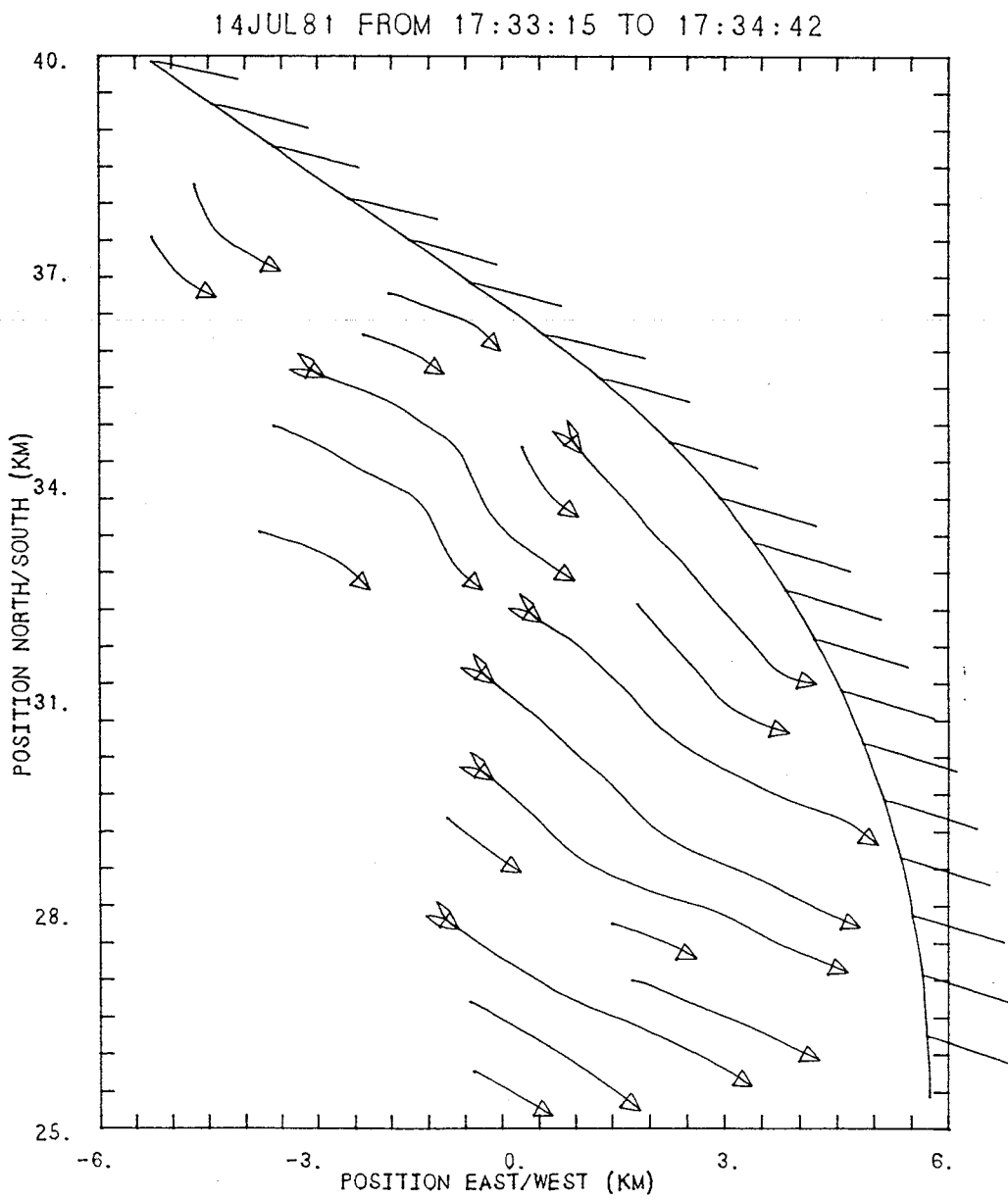
Fig. 12. The wind streamlines are computed for a selected portion of Fig. 2.
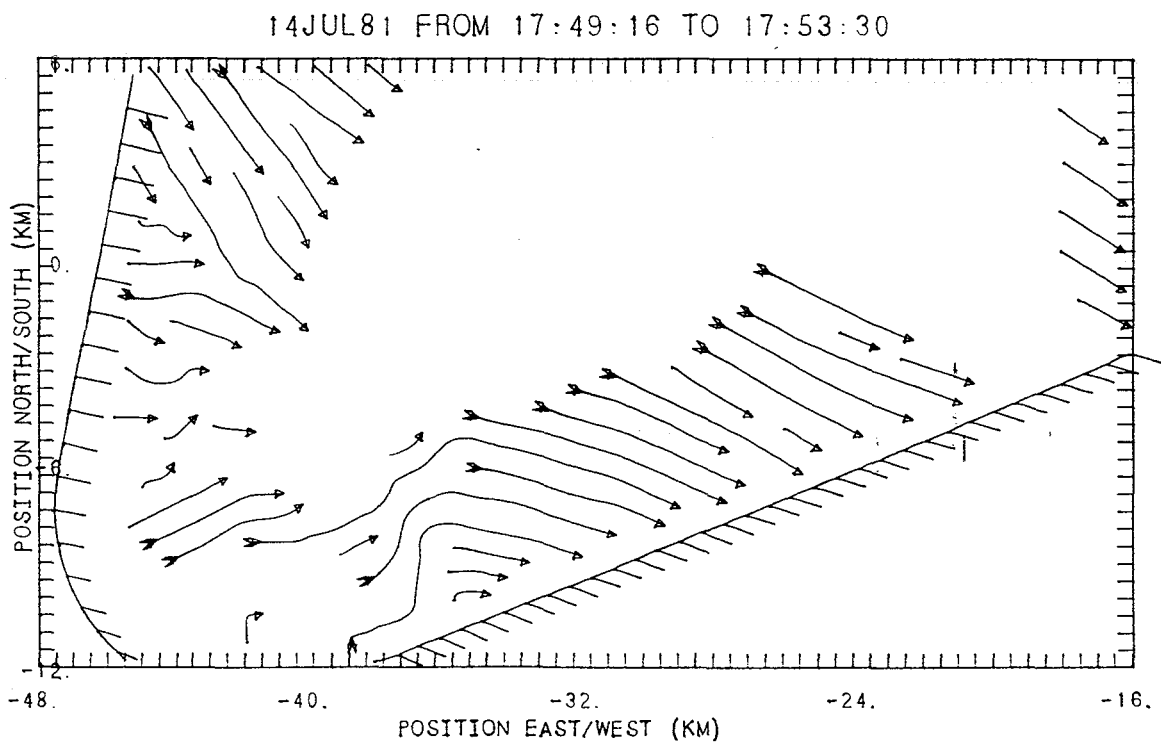
14JUL81 FROM 17:49:16 TO 17:53:30

Fig. 13. This shows wind streamlines computed for a portion of Fig. 4.

End of Document